A Comparative Study on the Fox and Lu Equations versus the Colored Stochastic Hodgkin-Huxley Equations

Liwaa Hussein AlObaidi

Submitted to the
Institute of Graduate Studies and Research
in partial fulfillment of the requirements for the Degree of

`

Master of Science
in
Computer Engineering

Eastern Mediterranean University
August 2013
Gazimağusa, North Cyprus

Approval of the Institute of Graduate Studies and Research

Prof. Dr. Elvan Yılmaz
Director

I certify that this thesis satisfies the requirements as a thesis for the degree of Master of Science in Computer Engineering.

Assoc. Prof. Dr. Muhammed Salamah
Chair, Department of Computer Engineering

We certify that we have read this thesis and that in our opinion it is fully adequate in scope and quality as a thesis for the degree of Master of Science in Computer Engineering.

Prof. Dr. Marifi Güler
Supervisor

Examining Committee

1. Prof. Dr. Marifi Güler _____

2. Assoc. Prof. Dr. Işik Aybay _____

3. Asst. Prof. Dr. Cem Ergün _____

ABSTRACT

In recent years, it has been argued and experimentally shown that ion channel noise in neurons can cause fundamental effects on the neuron’s dynamical behavior. Most profoundly, ion channel noise was seen to be able to cause spontaneous firing and stochastic resonance.

It was recently found by Güler (2011) that a non-trivially persistent cross correlation regarding position among the trans-membrane voltage fluctuations, and the element of open channel fluctuations is attributed to gate multiplicity. This non-trivial phenomenon was found to play an essential role in the elevation of excitability and spontaneous firing in the small size cell. Furthermore, the phenomenon was found to significantly enhance the spike coherence. More recently, the effect of the above cross correlation persistency was modeled by the same author Güler (2013), through inserting some colored noise terms inside the conductance's in the stochastic Hodgkin Huxley equation.

In this thesis, the broadly used stochastic of Hodgkin-Huxley equation, proposed by Fox and Lu, and the colored stochastic Hodgkin-Huxley equation, proposed by Güler recently, will be investigated in a comparative manner. The performance analysis of the two models will be performed with respect to the microscopic Markovain channel simulations. The statistic will be obtained using different membrane size and different input current values. Our investigation reveals that the performance of the Güler model is more effective than the Fox and Lu equations and gives better agreement with the microscopic simulation results.

Keywords: Channel Gate, Ion Channel, Small Size Membrane, Channel Noise, Stochastic Hodgkin-Huxley Equations.

ÖZ

Son yıllarda, nöronlardaki ion kanal gürültüsünün nöron dinamiği üzerinde hayati etki yapabildiği deneysel olarak da kanıtlanmıştır. Bu kapsamda, kendi kendine ateşleme ve stokastik rezonans en çarpıcı bulgulardır.

İyon kanallarında çoklu geçit bulunmasının, voltage dalgalanmaları ve açık kanal dalgalanmaları arasında ilk bakışta gözükmeyen bir daimi çapraz ilişkiye neden olduğu Güler (2011) tarafından ortaya çıkartılmıştır. Bu ilk bakışta gözükmeyen olgunun, küçük boyutlu hücrelerde yüksek uyarılma ve kendi kendine ateşlemeye neden olduğu bulunmuştur. Bu olgunun ateşlemede uyum artışı sağladığıda gözlenmiştir. Daha yakın zamanda, daimi çapraz ilişki, Hodgkin-Huxley denklemlerinde geçirgenliklere renkli gürültü terimleri ekleyerek modellenmiştir (Güler, 2013).

Bu tezde, yaygın olarak kullanılan Fox ve Lu'nun stokastik Hodgkin-Huxley denklemleri ve yukarıdaki renklendirilmiş stokastik Hodgkin-Huxley denklemleri karşılaştırmalı olarak incelenmiştir. Mikroskopik Markov benzeşim sonuçları referans alındığında, Güler modeli bulgularının Fox ve Lu bulgularından daha uyumlu olduğu gözlenmiştir.

Anahtar Kelimeler: Renkli Gürültü, Kanal Geçiti, İyon Kanalı, Küçük Boyutlu Zar, Kanal Gürültüsü, Stokastik Hodgkin-Huxley Denklemleri.

This thesis is dedicated to my lovely Parents,

Brothers and Sisters

For their endless love, support and encouragement

ACKNOWLEDGMENTS

First and foremost, I could like to thank Allah S.W.T for endowing me with health, patience, and knowledge to complete this thesis.

I sincerely acknowledge all the help and support that I was given by Prof. Dr. Marifi Güler whose knowledge, guidance, and effort made this research go on and see the light.

I have to thank my parents for their love and support throughout my life. Thank you both for giving me strength to reach for the stars and chase my dream. My brothers, my sisters, deserve my wholehearted thanks as well.

Special thanks go to my cousins Anas Kasim and Mustafa Ibrahim for their support and help.

Last but not least, I owe so much to my whole friends, for their understanding and encouragement in my many moments in crisis; our friendship makes my life a wonderful experience. I cannot list all the names here but you are always in my mind.

TABLE OF CONTENTS

ABSTRACT iii

ÖZ v

DEDICATION vi

ACKNOWLEDGMENTS vii

LIST OF FIGURES x

INTRODUCTION 1

1.1 Overview 3

NEURONS 4

2.1 Morphology and structure 4

2.1.1 What is an Action Potential? 6

2.1.2 Membrane proteins 6

2.1.3Synapses 7

2.2 Membrane Potential and Neuron Electrical Activity 9

HODGKIN - HUXLEY EQUATIONS 12

3.1 The Hodgkin-Huxley Model 12

3.1.1 The Ionic Conductance 14

DYNAMICS OF THE MEMBRANE 17

4.1 NCCP [The Non-Trivial Cross Correlation Persistency] 18

4.2 The Connection between NCCP and the Sodium Channels 23

4.3 Major impact of NCCP 24

THE COLORED NOISE MODEL FORMULATIONS 25

RESULTS AND DISCUSSION 27

6.1 Technologies Used: 29

CONCLUSION 44

REFERENCES 46

LIST OF FIGURES

Figure 1: Information Flow in a Neuron. 5

Figure 2: Synapses Examples. 9

Figure 3: Phases of an Action Potential 11

Figure 4: The Toy Membrane at Two Possible Conformational. 19

Figure 5: An Illustration of the Variation in the Voltage 22

Figure 6: Mean Spiking Rates Against the Input Current, Displayed by a Membrane Patch of 402 Potassium Channels and 1340 Sodium Channels. 29

Figure 7: The Coefficient of Variation Against the Input Current, Displayed by a Membrane Patch of 402 Potassium Channels and 1340 Sodium Channels 30

Figure 8: Mean Spiking Rates Against the Input Current, Displayed by a Membrane Patch of 801 Potassium Channels and 2670 Sodium Channels. 31

Figure 9: The Coefficient of Variation Against the Input Current, Displayed by a Membrane Patch of 801 Potassium Channels and 2670 Sodium Channels 32

Figure 10: Mean Spiking Rates Against the Input Current, Displayed by a Membrane Patch of 1002 Potassium Channels and 3340 Sodium Channels. 33

Figure 11: The Coefficient of Variation Against the Input Current, Displayed by a Membrane Patch Of 1002 Potassium Channels and 3340 Sodium Channels. 34

Figure 12: Mean Spiking Rates Against the Input Current, Displayed by a Membrane Patch Of 2700 Potassium Channels and 9000 Sodium Channels. 35

Figure 13: The Coefficient of Variation Against the Input Current, Displayed by a Membrane Patch Of 2700 Potassium Channels and 9000 Sodium Channels. 36

Figure 14: Mean Spiking Rates Against the Input Current, Displayed by a Membrane Patch of 3000 Potassium Channels and 10000 Sodium Channels. 37
Figure 15: The Coefficient of Variation Against the Input Current, Displayed by a Membrane Patch of 3000 Potassium Channels and 10000 Sodium Channels..... 38
Figure 16: Mean Spiking Rates Against the Input Current, Displayed by a Membrane Patch of 3500 Potassium Channels and 11670 Sodium Channels. 39
Figure 17: The Coefficient of Variation Against the Input Current, Displayed by a Membrane Patch of 3500 Potassium Channels and 11670 Sodium Channels..... 40
Figure 18: Mean Spiking Rates Against the Input Current, Displayed by a Membrane Patch of 4002 Potassium Channels and 13340 Sodium Channels.. 41
Figure 19: The Coefficient of Variation Against the Input Current, Displayed by a Membrane Patch of 4002 Potassium Channels and 13340 Sodium Channels..... 42
Figure 20: Spontaneous Firing, Displayed by a Membrane Patch of 801 Potassium Channels and 2670 Sodium Channels 43

Chapter 1

INTRODUCTION

The effect of noise to the neurons produces an unusual pattern on the neuronal dynamics. There are two types of noise; internal and external (Faisal A. S., 2008). External noise arises from synaptic signal transmission, while internal noise is specific to the cell. The existence of a finite number of ion channels in a patch of neuronal membrane is the major source of internal noise. The prime source of internal noise in a neuronal membrane spot is from the limited number of voltage-gated ion channels. The number of open channels fluctuates in a seemingly random manner (Sakmann &Neher, 1995) implying a fluctuation in the conductivity of the membrane, which, in turn, implies a fluctuation in the transmembrane voltage. (Sakmann, 1995). If fluctuations are included in the membrane conduct, then fluctuation will be included in the voltage of transmembrane as well. When the number of ion channels is large this means that the membrane size is huge, the voltage dynamics will represent as in the original Hodgkin and Huxley (Hodgkin, 1952) equation. However, when the patch of membrane is small, the conductance fluctuations affect the voltage activity of the cell. These effects are probably important and cannot be ignored. The single open channel stochastically it effect in a direct manner the spike behavior which is suggested by experiment investigation ((Sigworth, 1980); (Lynch, 1989); (Johansson, 1994)), and spontaneous fire will be the result of that noise in the ion channels ((Koch, 1999);(White, 1998)).

Patch-clamp experiments in vitro have demonstrated that the noise of channel in the dendrites also in the soma resulting voltage fluctuations that are large enough to affect asynchronies in the timing, initiation, and propagation of action potentials ((Diba, 2004); (Jacobson, 2005); (Dorval, 2005); (Kole, 2006);). The phenomenon called stochastic resonance has been observed to occur in a system of voltage-dependent ion channels formed by the peptide alamethicin ((Bezrukov, 1995)).

Spontaneous spiking is a phenomenon caused by the internal noise from the ion channels. Proof through theoretical investigations and numerical simulations of channel dynamics (in the form of repetitive spiking or bursting), or in otherwise quiet membrane patches ((DeFelice, 1992); (Strassberg, 1993); (Chow, 1996); (Rowat, 2004); (Güler, 2007) ;(Güler, 2008);(Güler, 2011); (Güler, 2013); (N. A. Kako, 2013)); furthermore, have revealed the occurrence of stochastic resonance and the coherence of the generated spike trains ((Jung, 2001); (Schmid, 2001); (Özer, 2006)). Even in the presence of large numbers of ion channels, channel fluctuations can become critical near the action potential threshold ((Schneidman, 1998); (Rubinstein, 1995)); the timing precision of an action potential is determined by the small number of ion channels that are open at the action potential threshold. It has also been shown that spike propagation in axons is affected from ion channel noise ((Faisal A. A., 2007); (Ochab-Marcinek, 2009); (Omer Hayman F., 2013)).

It has been revealed in earlier theoretical experiments (Güler. 2011) that it is not just the gate noise (the quantity of fluctuations in the open gates) that affects neuron's behavior, but also the existence of a large quantity of gates in single ion channel, Furthermore this

effect that may be pointing on an important role in activity within the cell in case of having membrane bounded in size. More recently, a stochastic Hodgkin – Huxley model, having colored noise terms in the conductance was proposed (Güler, 2013), where the colored terms capture those effects due to the gate multiplicity.

1.1 Overview

In this dissertation, the colored stochastic Hodgkin Huxley equations, introduced by Güler (2013) are going to be compared with the Fox and Lu equations and microscopic simulations. Particularly, the performance analysis of the two models will be performed with respect to the microscopic Markovain channel simulations. Chapter one contains the introduction, Chapter two handles neuron morphology and structure, in Chapter three the Hodgkin Huxley equation is dealt with. Chapter 4 contains the membrane dynamics, whereas; Chapter 5 includes Güler model formulations and Chapter 6 includes the experiments and results of the study.

Chapter 2

NEURONS

2.1 Morphology and structure

The most important cell responsible for brain function is the neuron. There are about 100 billion neurons in the brain. It has a unique ability to transfer electrical signals to over long distances in the body. Neurons are nerve cells in nature; therefor it transmits nerve signals to and from the brain at up to 200 mph. The neuron consists of a cell body (or soma) with branching dendrites (signal receivers) and a projection called an axon, which conducts the nerve signal. At the other end of the axon, the axon terminals transmit the electro-chemical signal across a synapse (the gap between the axon terminal and the receiving cell) as shown in figure (1). The axon is a long extension of a nerve cell, and takes information away from the cell body.

In the brain of the mouse, the cortical neurons have been estimated that the length of axon is equal to about 40 mm and has in its branches almost four mm of total dendrite. Each axon makes connections of nearly 180 per µm synaptic connection with other branches of dendrite, which is a part of the other neurons. Furthermore, each dendritic tree receives an average of two signals per µm from another. The soma of ideal cortical neurons reaches in diameter from 10 up to 25 µm. (Abbot, 2010).

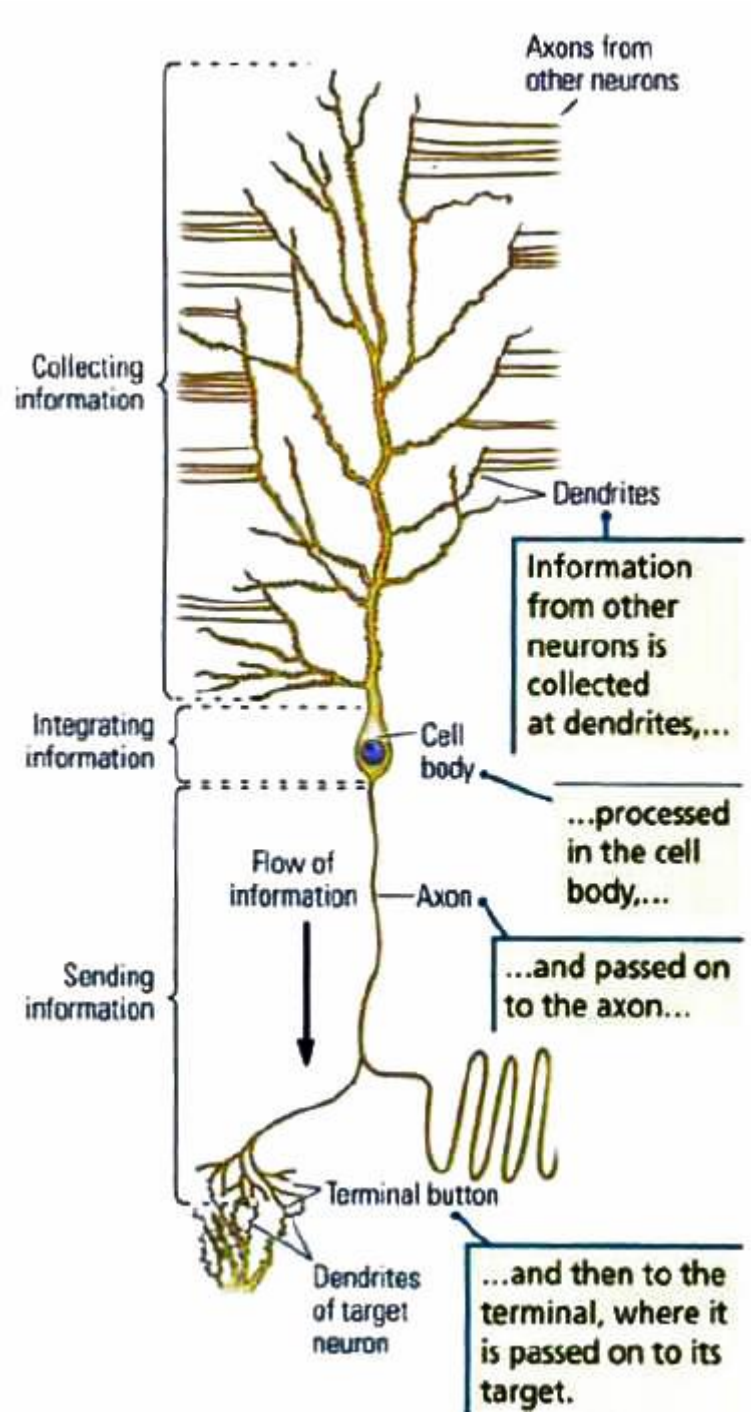

Figure 1: Information Flow in a Neuron (Kolb and Whishaw 2009)

2.1.1 What is an Action Potential?

Neurons play a central role in cell-to-cell communication process, where the cell may receive information from 1,000 other passing signals to each other via as many as 1,000 trillion synaptic connections. Via a synapse from another neuron, electrical signal received causes the trans-membrane current, which works to change the membrane potential or cell voltage. This signal that comes from synaptic is called the post synapse potentials (PSPs), little current generates tiny PSPs, large current means considerable PSPs. Voltage sensitive channel embedded in a neuron is amplified to result in generation of spike or action potential (Izhikevich, 2007).

2.1.2 Membrane proteins

Each neuron cell contains proteins specialized to move materials through other. In order to understand many neurons functions, some facts about these proteins are needed. They can be classified into three groups in accordance with how these proteins assist in transporting the materials in the membrane. Each kind of protein's function has the capability to change its form according to that function.

2.1.2.1 Channels

It is just membrane protein which is produced in a variety of channels or holes, allowing some materials to pass through. The size of the channel varies depending on the function of that channel. So, small sized holes control little sized substances to pass through in or out into the cell and the same many different sizes of substances. There are protein molecules working as a channel like sodium (NA+), potassium (K+), calcium (Ca2+), and chloride (Cl-).

2.1.2.2 Gates

One of the important protein's molecules features is that they have special ability to change their shape. These proteins are known as gates. The function of the gates is always to allow some or specific chemicals to pass through and bind with others. These implanted proteins behave as being a pass. They can be active when the chemical correspond with the embedded proteins by the shape and the size, and there are numerous types of gate responses to various motivations, for example, electrical charge or temperature change to allow the certain chemical to cross.

2.1.2.3 Pump

There is another kind of membrane proteins which is modified to operate like a pump, moving substances around the membrane in accordance with energy requirements for the transporter molecule. For instance; proteins shaping their pattern in a state to pump particular ions, like Na+ ions are transferred in one side and K+ ions will be transferred to other side. Additionally, protein pump transports many other substances.

2.1.3 Synapses

Synapses are designed just like a junction between two consecutive neurons in the event when the axon of sensory neuron is coupled to the efferent one and grants a method to carry the data to other cell axon’s end at the synapses. The voltage passing over the action potential opens ion channels developing a stream of Ca2+ which will produce a neurotransmitter to release. Receptors bind the neurotransmitter on the signal receiving or post synaptic side for synapse ultimately causing the opening of ion-conducting channels. According to the ion flow’s nature, the synapses may have inhibitory,

depolarizing, or excitatory, typical hyper-polarizing, effects on the post synaptic neuron (Dayan and Abbot 2002).

Synapses are certainly not scattered randomly above the external top of the dendrite. In general, inhibitory synapses are proximally more than excitatory synapses, even though they also exist at distal dendrite regions when present on several spines in mixture with an excitatory input (Segev in Bower and Beeman 2003). In numerous systems (e.g., Cerebellar Purkinje and pyramidal hippocampal cells), an input source given is preferential planned onto a certain region inside the dendritic tree (Shepherd 1990), as an alternative to being randomly scattered above the external surface of the dendrite. Electron micrographic images of synapses in neurons are shown in figure (2).

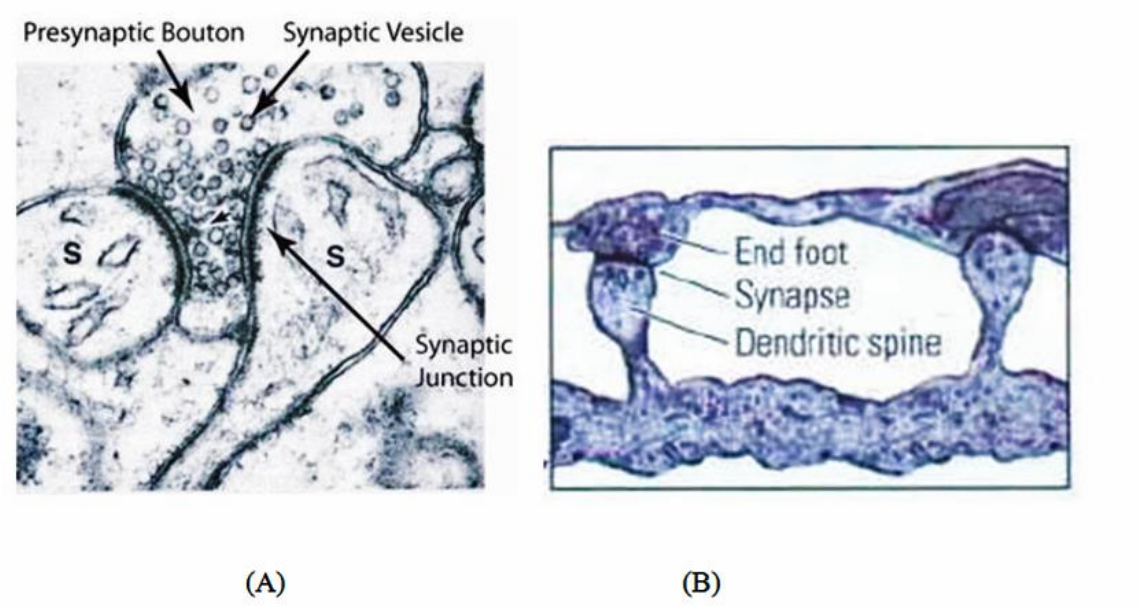

Figure 2: Synapses Examples: (A) Electron Micrograph of Excitatory Spiny Synapses (S) Shaped on the Dendrites of a Rodent Hippocampal Pyramidal Cell. (B) An Electron Micrographic Figure Captures the Synapse Formed Where the Terminal Bottom of One Neuron Meets a Dendritic Spine on a Dendrite of Another Neuron (Kolb And Whishaw 2009)

2.2 Membrane Potential and Neuron Electrical Activity

Membrane potential is referred to as the real difference in electrical potential amongst the interior and extracellular fluid (ECF) of the neuron. Under resting situation, the potential of the cell membrane inside of a neuron is around -70 mV in accordance with the nearby areas. That voltage, nevertheless, is traditionally assumed to become zero mV for convenience, and also the cell state is considered to be polarized. This potential is an equilibrium spot where the ions that flow into the cell equal to those which flow out of the cell. This potential of the membrane difference is sustained by ion pumps found in the cell membrane by maintaining focus on gradients. For example, concentration of Na+ inside the extracellular of any neuron is a lot more than inside it, and the K+ concentration in a neuron is significantly higher inside than the nearby fluid. Because of

this, the flow of ions gets into and out of a cell due to voltage and concentration gradients through the cell state of transition.

Latest, such electropositive ions flowing out from the cell (or maybe electronegative ions flowing in the cell) over open channels make the membrane potential more negative, an operation called hyper-polarization. Current streaming in the cell diminishes the negativity of the membrane potential or even causes it to become positive values. This is called de-polarization. The membrane potential will rise above a threshold level like a neuron. De-polarization is large enough to rise, a process with positive feedback will start and the neuron creates an action potential, which are nearly 100 mV fluctuations inside the electric potential passing over the membrane cell that takes about 1ms.

Once an action potential occurs, it is impossible to trigger another spike directly after the earlier one, and this is referred to as the absolute refractory period. The significance of action potential is that different sub-threshold fluctuations that attenuate over distance of as a matter of fact 1 millimeter. They are able to propagate over large distances without attenuation along axon processes (Dayan and Abbot 2002). Figure (3) explains the neuron voltage dynamic while an action potential that is tuned by way of a corresponding ion channel activity. With this figure, the resting potential is in its real value of -70 mV.

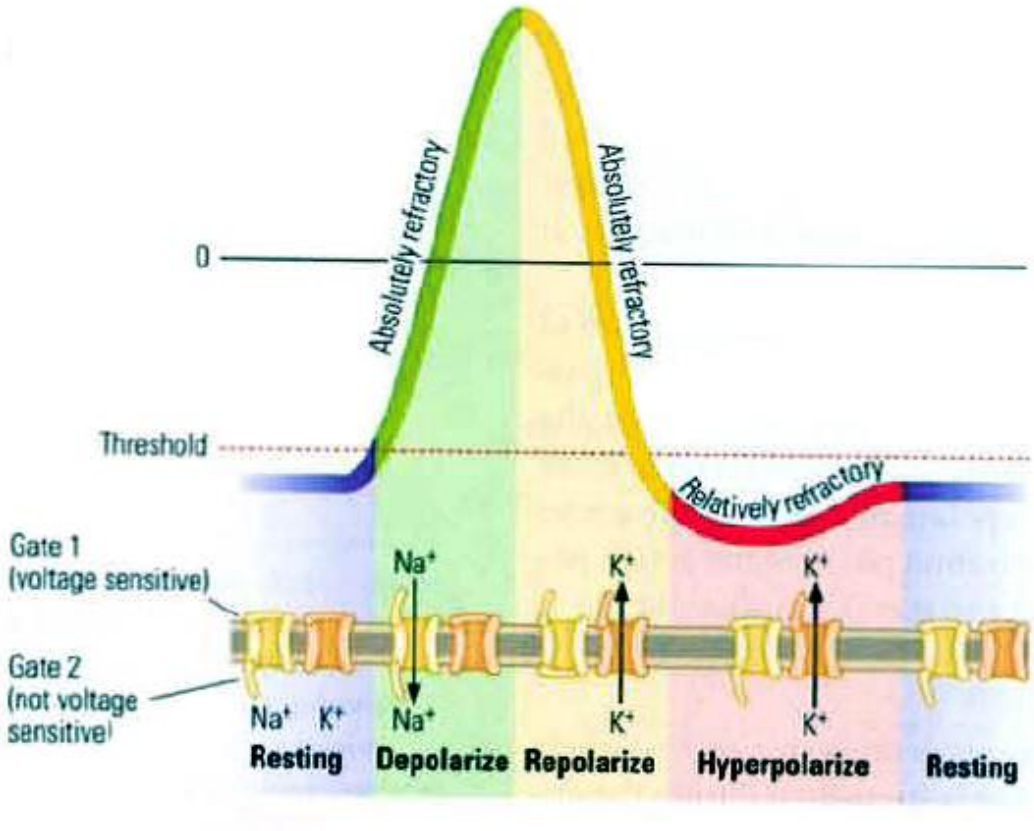

Figure 3: Phases of an Action Potential Initiated by Changes in Voltage Sensitive Sodium and Potassium Channels; an Action Potential Begins with a Depolarization (Gate 1 of the Sodium Channel Opens and Then Gate 2 Closes). The Slower-Opening Potassium Channel Contributes on Re-Polarization and Hyper-Polarization until the Resting Membrane Potential is Restored (Kolb and Whishaw 2009)

Chapter 3

HODGKIN - HUXLEY EQUATIONS

During the last years, plenty of neural models for several needs have been located and developed. Moreover, the variety of these models depends on the structurally realistic biophysical model. As an illustration, the most significant models over time is the Hodgkin – Huxley (HH) equations, and the one which this thesis concentrates on the Color Noise model (located by Prof. Dr. Marifi Güler) and that is, in reality, applying the (HH) model to become more accurate if compared with the exact neuron. Different models may be required in numerous studies in accordance with biological properties of models, complication as well as implementation cost. On the other hand, modeling technique of neural excitability was attached through the work of Hodgkin-Huxley (1952). The Hodgkin – Huxley model will be explained shortly in this chapter.

3.1 The Hodgkin-Huxley Model

According to experimental research accomplished on an axon of giant squid by applying space clamp and voltage clamp techniques, Hodgkin and Huxley (HH) (1952) argued that the current passing from the axon of any squid only has two major ionic elements, I_{Na} and I_K (sodium and potassium channel equivalent elements). The membrane potential V_m has an impact upon these currents appreciably. Consequently, using their observation, they developed a mathematical model to generate a model which is still one

of the most essential models and significant, researchers have developed many of reasonable neural models (Hodgkin and Huxley 1952).

In this model, the electrical qualities of any section of nerve membrane that may be graven by an equivalent circuit in a way that current passing from the membrane has two key elements, the first one is related to charging the membrane capacitance and the second one is related to particular kinds of ion's movement by means of membrane. And then, the ionic current is additionally split into three recognizable currents, sodiumI_{Na}, potassiumI_K, and small leakage I_L which is mostly conveyed by chloride ions.

The differential equation that refers for the electrical circuit is shown below:

$$C_m \frac{dV_m}{dt} + I_{ion} = I_{ext} \quad (1)$$

Where C_m is membrane capacitance, V_m is membrane potential, and I_{ext} is the current that externally applied. I_{ion} is ionic current passing through the membrane and can be calculated from the next equation:

$$I_{ion} = \sum_i I_i \quad (2)$$

$$I_i = g_i(V_m - E_i) \quad (3)$$

I_i shows each ionic element which has related conductance g_i and reversal potential E_i.

In the model of a massive squid axon, it has three forms of currents (I_i): sodiumI_{Na}, potassiumI_K, and leakage I_L and which will provide us this equation:

$$I_{ion} = I_{Na} + I_K + I_L = g_{Na}(V_m - E_{Na}) + g_K(V_m - E_K) + g_L(V_m - E_L) \quad (4)$$

The macroscopic $g_i(g_{Na}, g_K, g_L)$ conductance begins in the united influence of the large amount of membrane microscopic ion channels. Ion channel can be viewed as physical gates in a tiny number that manage the ions flow along the channel. While each of the gates within an ion channels are usually in the permissive condition, ions can flow over the channel, plus the channel is open.

3.1.1 The Ionic Conductance

Ions can move across the channel which is open while every one of the gates for a certain channel is in the permissive state. The formal presumptions accustomed to illustrate the potassium and sodium conductance through empirical observation attained by voltage clamp experiments are:

$$g_K = \bar{g}_K n^4 \tag{5}$$

$$g_{Na} = \bar{g}_{Na} m^3 h \tag{6}$$

Where n, m and h are variable's dynamics in the ion channel gate which will be shown subsequently, $\bar{g}_i$ is a constant with the scales of conductance per cm^2 (keep in mind that n is between 0 and 1, accordingly, the absolute maximum conductance value ($\bar{g}_i$) is necessary to normalize the actual result).

The dynamics of n, m and h are shown below:

$$\dot{\mathrm{n}} = \frac{\mathrm{dn}}{\mathrm{dt}} = \alpha_{\mathrm{n}}(1 - \mathrm{n}) - \beta_{\mathrm{n}}\mathrm{n} \tag{7}$$

$$\dot{\mathrm{m}} = \frac{\mathrm{dn}}{\mathrm{dt}} = \alpha_{\mathrm{m}}(1 - \mathrm{m}) - \beta_{\mathrm{m}}\mathrm{m} \tag{8}$$

$$\dot{\mathrm{h}} = \frac{\mathrm{dh}}{\mathrm{dt}} = \alpha_{\mathrm{h}}(1 - \mathrm{h}) - \beta_{\mathrm{h}}\mathrm{h} \tag{9}$$

where α_x and β_x are rate constants, that change with voltage not in the time, n is really a non-dimensional variable that can fluctuate among 0 and 1 as well as shows the individual gate possibility of being in the permissive state.

In test on voltage clamp, the membrane potential will begin rest state at (V_m = 0), after that it promptly changes to a new voltage clamp $V_m = V_c$. The answer to Eq. (1) is a simple exponential shown below:

$$x(t) = x_\infty(V_c) - \big(x_\infty(V_c) - x_\infty(0)\big)\exp(-t/\tau_x) \tag{10}$$

$$x_\infty(0) = \alpha_x(0)/\alpha_x(0) + \beta_x(0) \tag{11}$$

$$x_\infty(V_c) = \alpha_x(V_c)/\alpha_x(V_c) + \beta_x(V_c) \tag{12}$$

$$\tau_x(V_c) = [\alpha_x(V_c) + \beta_x(V_c)]^{-1} \tag{13}$$

where x represents time based upon gating variables n, m and h .To make this formula less complicated , $x_\infty(0)$ and $x_\infty(V_c)$ symbolizes gating variables value at standard rest state voltage 0 and clamped voltage V_c . τ_x Represents the fixed time course to realize the steady-state value of $x_\infty(V_c)$ in the event the voltage clamped to V_c .

The fixed α_i and β_i are calculated in Hodgkin and Huxley as functions of V as follows:

$$\alpha_i = \frac{x_\infty(V)}{\tau_n(V)} \tag{14}$$

$$\beta_i = \frac{1 - x_\infty(V)}{\tau_n(V)} \tag{15}$$

As I've already explained i is an index representative for n, m, and also h variables in the ion channel gate. The rates expressions of constants α_i and β_i which are experimentally completed are shown as follows:

$$\alpha_n(V) = \frac{0.01(10-V)}{\exp\left(\frac{10-V}{10}\right)-1}, \tag{16}$$

$$\beta_n(V) = 0.125\, exp\left(-\frac{V}{80}\right), \tag{17}$$

$$\alpha_m(V) = \frac{0.1(25-V)}{exp\left(\frac{10-V}{10}\right)-1}, \tag{18}$$

$$\beta_m(V) = 4\, exp\left(-\frac{V}{18}\right), \tag{19}$$

$$\alpha_h(V) = 0.07\, exp\left(-\frac{V}{20}\right), \tag{20}$$

$$\beta_h(V) = \frac{1}{exp\left(\frac{30-V}{10}\right)+1} \tag{21}$$

All of $\alpha(V)$ and $\beta(V)$ describe the transition rates between open and closed states of the channels.

Chapter 4

DYNAMICS OF THE MEMBRANE

The transmembrane voltage V evolves in time in accordance with the differential equation:

$$C\,\frac{dV}{dt} = -g_K\psi_k(V_m - E_K) - g_{Na}\psi_{na}(V_m - E_{na}) - g_L(V_m - E_L) + I \qquad (22)$$

Also ψ_K is a dynamic variable from the formula which signifies the number of open channel from potassium that is the relative amount of open channel towards the complete number of potassium channel inside the membrane; furthermore ψ_{Na} is open sodium channels ratio. Every one of the constant parameters value of the membrane utilized in Eq. (22) can be found in below. Each of the two channel variables ψ_K and ψ_{Na} inside the Hodgkin – Huxley (HH) equations obtains its own estimated deterministic value, $\psi_K = n^4$ and $\psi_{Na} = m^3h$; whilst potassium channel has four n-gates and sodium channel has three m-gates and one h-gate. Just in case the channel is regarded as open, all channel gates must become open, as well as the gating variable for potassium is *n* and for sodium is *m* and *h*. So, N_K and N_{Na} matched to the whole numbers of channels for potassium and sodium. To obtain the complete amount of open channels, the N_K ought to be simply multiplied by 4n for potassium for getting $4N_Kn$ plus sodium resulting $3N_{Na}m$, $N_{Na}h$. Alternatively, the Markov process has been put into the gates dynamics.

The chance of an n-gate is closed relating to the time t whilst still closed or gets open when time t+Δt is $exp(-\alpha_n \Delta t)$, along with the possibility of being open at time *t*, and continues to be open when time $t + \Delta t$ is $exp(-\beta_n \Delta t)$ which means that every one of the parameters α_n and β_n are classified as the rate of voltage-dependent opening and closing of n-gates. Likewise, the same process is implemented for the m-gate and h-gate. The rate functions are found to be:

$$\alpha_n = (0.1 - 0.01V)/(exp(1 - 0.1V) - 1), \quad (23a)$$

$$\beta_n = 0.125 \exp(-V/80), \quad (23b)$$

$$\alpha_m = (2.5 - 0.1V)/(exp(2.5 - 0.1V) - 1), \quad (23c)$$

$$\beta m = 4\, exp(-V/18), \quad (23d)$$

$$\alpha h = 0.07\, exp(-V/20), \quad (23e)$$

$$\beta h = 1/(exp(3 - 0.1V) + 1). \quad (23f)$$

4.1 NCCP [The Non-Trivial Cross Correlation Persistency]

As mentioned before, the potassium channel has several n-gates inside it and also in the event the proportions of open gates are identified, it isn't sufficient to fulfill ψ_K. For example, a membrane that includes couple of potassium channels (eight gates), possibly in the case of time at t_2, may point out that one among the two channels has all its open gates even though the other channel has only two open gates. On the other hand, within a different period of time t_1, every one of the channel has got the same number of open gates, so this means that even that membrane has equal number of open gates through the two periods of time, one of the two channels is open in moment t_2 but there are no channels at moment t_1 see Fig.(4), although the term gate-to-channel uncertainness identifies this problem of knowledge which is put in ψ_K and in some cases

if n is known and also the expression gate noise is important during these random fluctuations in n (Güler, 2011).

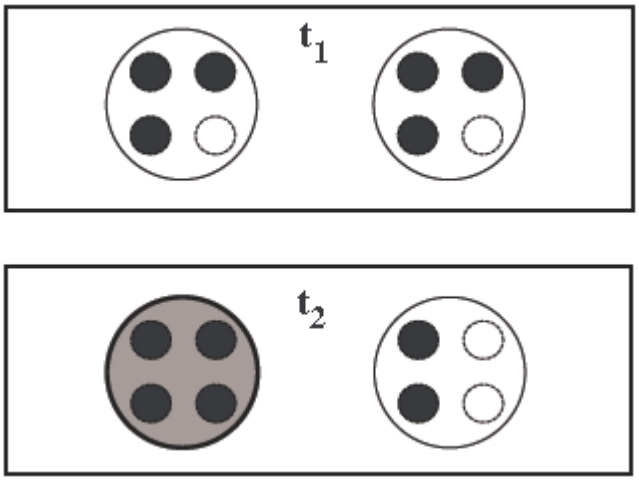

Figure 4: the toy membrane at two possible states (Güler, 2011)

The gate-to-channel is known as dynamic random fluctuations inside the construct $\psi_K - [\psi_K]$; from this construct the channel fluctuations which appear from the gate-to-channel uncertainty are bounded. When the gate-to-channel uncertainty didn't exist, the construct could possibly be vanishing no matter the gate noise. Here $[\psi_K]$ is framed for that arrangement mean in the ratio of open potassium channels; measured via all achievable arrangement in the membrane getting $4N_K n$ open n-gates, as shown below:

$$[\psi_K] = \frac{(4N_K n - 3)(4N_K n - 2)(4N_K n - 1)n}{(4N_K n - 3)(4N_K n - 2)(4N_K n - 1)}\ , if\ N_K n \geq 1 \qquad (24)$$

$[\psi_K]$ = 0 for else. Next the construct $\psi_K - [\psi_K]$ will assess the distinction between numbers of open channels through the arrangement mean at any time. Unless the membrane is extremely tiny in size, it's going to be $[\psi_K] \approx n^4$. In the event of finite membrane but limitless in size, the construct fluctuations will vanish. So, when

membranes are large, the HH value to get used is $\psi_K = [\psi_K] = n^4$ at any time. The construct might be unnecessary in another condition when all the channels just have one gate open, no matter the membrane size was, so in fact we will have $\psi_K = [\psi_K] = n$.

Concepts of the order parameters Ω_K^V and Ω_K^n as the given cross correlations are going to be:

$$\Omega_K^V = \frac{\big((\psi_K - [\psi_K])V\big) - (\psi_K - [\psi_K])(V)}{([\psi_K])(n)} \tag{25}$$

$$\Omega_K^n = \frac{\big((\psi_K - [\psi_K])n\big) - (\psi_K - [\psi_K])(n)}{([\psi_K])(n)} \tag{26}$$

Here the expectation values $< \cdot \ \cdot >$ are merely the foundation averages above the membrane conformation condition and all of these conformation conditions are related to time. Separately from each other's, through using Markovian process of the consisting gate condition and in equation (22); the ensemble during $t + \Delta t$ is set from the starting moment t, to satisfy suitability of the scale and the dimensionality these terms are included. Ω_k^v is a measure of the correlation between the fluctuations of the construct $\psi_K - [\psi_K]$ and the fluctuations of the voltage V . Ω_k^n is almost the same, controlling the fluctuations of n instead of V. This is due to the fact that the construct positivity or negativity is going completely irregular and uncontrollable by any of the fluctuations of V or n . After an initial passing moment, it becomes easy to predict that the order parameters decrease to none and this initiation is wrong in both the theoretical arguments and the numerical experiments of the channels. However, according to the simulations for near-equilibrium dynamics, the order parameter becomes and continues less than zero within the phase of sub-threshold actions. A non-trivially continual

correlation reserves a position between the fluctuations of V and the fluctuations of the construct $\psi_K - [\psi_K]$ and also the fluctuations of n, and this phenomenon is what NCCP pointing on.

It is really possible that these order parameters remain not zero as specified by Markovian evaluation in that the condition in the gate at moment $t + \Delta t$ relies on the condition at moment t: even when the penetration of dependence declining while using the interval in Δt is larger. Meaning, the construct $\psi_K - [\psi_K]$ has not received a disappearing autocorrelation function and the time with the autocorrelation is fixed and should not reach to zero. Thus, leading the plus value of $[V - E_K]$ becomes useful .This means you will be removed from the equation (17) from the condition that $\psi_K - [\psi_K]$ is greater than zero during some time frame, after that a poor variance appearing in dV/dt as well as that period. At this point, the variance is based on having the construct $\psi_K - [\psi_K]$ adequate to home in the same duration, and from that this variance turns to negative for the reason that period. Those rentals are portrayed by:

$$\psi_k - [\psi_k] > 0 \Rightarrow \delta\left(\frac{dV}{dt}\right) < 0 \Rightarrow \delta V < 0 \tag{27}$$

Moreover, the variation within the situation of negative $\psi_K - [\psi_K]$ was shown as:

$$\psi_k - [\psi_k] < 0 \Rightarrow \delta\left(\frac{dV}{dt}\right) > 0 \Rightarrow \delta V > 0 \tag{28}$$

Inside the two above equations, (27) and (28), if your sign of $\psi_K - [\psi_K]$ just isn't considered, the additional value of $(\psi_K - [\psi_K])\delta V$ is minus during the all-time fainting making $\psi_K - [\psi_K]$ not visiting a positive. A graphical demonstration shown in Fig (5)

clarifies that the dwelling time of $\psi_K - [\psi_K]$ in the same of algebraic sign must not be less than the duration of the actual fluctuation in V.

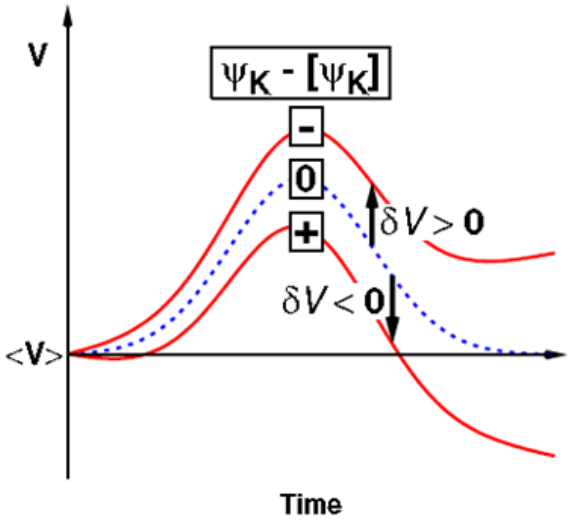

Figure 5: An illustration of the variation in the voltage, denoted by δV, in response to deviations of the construct $\psi_K - [\psi_K]$ from zero. (Adopted from (Güler, 2011))

In addition, should the sign in the product $\psi_K - [\psi_K]$ is switched during the time scale, the value of the previous case won't become below zero again at any time; for the short moment directly following, the sign turned results in getting a new sign to positive. In case the dwelling period is assumed remarkably greater than the repose time in the $\psi_K - [\psi_K]$ for being below zero again, the chances of the output in negative is going to be bigger than picking out the product in positive. As a result, the voltage fluctuations V will likely be negatively correlated while using the fluctuations of $\psi_K - [\psi_K]$. Therefore, the configuration variable Ω_v^k will reach minus value. The fluctuations, long-lasting only for a microscopic time window, enforce order at macroscopic time window.

Furthermore, on the list of reasons that an order parameter Ω_n^k values will not become zero, could be that the deference of variation δV from V, while using the deviations from $\psi_K - [\psi_K] = 0$. Each of the rates α_n and β_n are voltage relevance function that increases while using the voltage. Since an increase in α_n decreases the expectation of the closed n-gate staying closed plus a lowering of β_n increases the probability of a wide open n-gate being open, a good δV makes a positive alternation in the gating inconstant n. This progress, much like Ω_v^k, Ω_n^k also achieves a damaging value.

4.2 The Connection between NCCP and the Sodium Channels

The notion that displays the gate-to-channel uncertainty connected with the sodium channels is $\psi_{Na} - [\psi_{Na}]$. After all this, the structure medium of the ratio of open sodium channels, $[\psi_{Na}]$ becomes:

$$[\psi_{Na}] = \frac{(3N_{Na}m - 2)(3N_{Na}m - 1)m}{(3N_{Na} - 2)(3N_{Na} - 1)}h, \;\; if\; N_{Na}m \geq 1 \tag{29}$$

$[\psi_{Na}] = 0$, else only the membrane is quite tiny in proportions, to thought to be:

$$[\psi_{Na}\,] \approx m^3 h \tag{30}$$

Once we employ a set membrane with infinite size, the HH value $\psi_{Na} = [\psi_{Na}] = m^3 h$ assigns constantly. The principle order variable relating to the sodium channels Ω_{Na}^v is provided by:

$$\Omega_{Na}^V = \frac{\big((\psi_{Na} - [\psi_{Na}])V\big) - (\psi_{Na} - [\psi_{Na}])(V)}{([\psi_{Na}])(E_{Na} - E_K)} \tag{31}$$

The simulations showing that Ω_{Na}^v gets positive values and constantly remains to be in positive, inside the phase of sub-threshold action. This can be only reserved for the near-

equilibrium dynamics, a non-trivially continual correlation gets placed within the fluctuations in the construct $\psi_{Na} - [\psi_{Na}]$ as well as the changes of V remarking which the sign of Ω_{Na}^{v} is conflicting with all the sign of Ω_{k}^{v} . It is because of the signs of $V - E_k$ and $V - E_{Na}$ in equation (22) are opposite at any moment, the prior is positive and also the final is negative.

4.3 Major impact of NCCP

It turned out as expected that the increases from the diversity with the amplitude of sub-threshold voltage fluctuations originate from the NCCP, which is through increasing the possibility of fluctuations with bigger amplitudes and that is covered in detail in Güler, 2013. And then, it demonstrated that the diversity to produce easier with the cell's spiking through forcing the passing on the firing to the sub-threshold phase has grown to be simpler. On the other hand, it had been found that limited scale membranes beholden their upraised irritability not only to the gate noise but, into a larger range, as well as to NCCP. Furthermore, NCCP was noticed to further improve the consistency in spiking.

Chapter 5

THE COLORED NOISE MODEL FORMULATIONS

The colored stochastic Hodgkin Huxley equations (Güler, 2013) are given by:

$$CV = g_K\psi_K(V - E_K) - g_{Na}\psi_{Na}(V - E_{Na}) \tag{32}$$

$$-g_L(V - E_L) + I \tag{33}$$

$$\psi_K = n^4 + \sqrt{\frac{n^4 - (1 - n^4)}{\mathrm{N_K}}\, q_K} \tag{34}$$

$$\psi_{N_a} = m^4\mathrm{h} + \sqrt{\frac{m^3 - (1 - m^3)}{\mathrm{N_{N_a}}}\, hq_{\ K}} \tag{35}$$

$$\tau\dot{\mathrm{q}}_{\mathrm{K}} = \mathrm{p_K}, \tag{36}$$

$$\tau\dot{\mathrm{p}}_{\mathrm{K}} = -\gamma_{\mathrm{K}}\mathrm{p_K} - \omega_{\mathrm{K}}^2[\alpha_{\mathrm{n}}(1 - \mathrm{n}) + \beta_{\mathrm{n}}n]\mathrm{q_K} + \xi_{\mathrm{K}}, \tag{37}$$

$$\tau\dot{\mathrm{q}}_{\mathrm{Na}} = \mathrm{p_{Na}}, \tag{38}$$

$$\tau\dot{\mathrm{p}}_{\mathrm{Na}} = -\gamma_{\mathrm{Na}}\mathrm{p_{Na}} - \omega_{\mathrm{Na}}^2[\alpha_{\mathrm{m}}(1 - \mathrm{m}) + \beta_{\mathrm{m}}m]q_{Na} + \xi_{\mathrm{Na}} \tag{39}$$

$$\dot{\mathrm{n}} = \alpha_{\mathrm{n}}(1 - \mathrm{n}) - \beta_{\mathrm{n}}\mathrm{n} + \mathrm{n_n} \tag{40}$$

$$\dot{\mathrm{m}} = \alpha_{\mathrm{m}}(1 - \mathrm{m}) - \beta_{\mathrm{m}}\mathrm{m} + \mathrm{n_m} \tag{41}$$

$$\dot{\mathrm{h}} = \alpha_{\mathrm{h}}(1 - \mathrm{h}) - \beta_{\mathrm{h}}\mathrm{h} + \mathrm{n_h} \tag{42}$$

where, the Gaussian white noise terms have zero means and their mean squares obey :

$$[\xi_K(t)\xi_K(t')] = \gamma_K T_K[\alpha_n(1-n) + \beta_n n]\delta(t-t') \quad (43)$$

$$[\xi_{Na}(t)\xi_{Na}(t')] = \gamma_{Na} T_{Na}[\alpha_m(1-m) + \beta_m m]\delta(t-t') \quad (44)$$

$$[\eta_n(t)\eta_n(t')] = \frac{\alpha_n(1-n) + \beta_n n}{4N_K}\,\delta(t-t') \quad (45)$$

$$[\eta_m(t)\eta_m(t')] = \frac{\alpha_m(1-m) + \beta_m m}{3N_{Na}}\,\delta(t-t') \quad (46)$$

$$[\eta_h(t)\eta_h(t')] = \frac{\alpha_h(1-h) + \beta_h h}{N_{Na}}\,\delta(t-t') \quad (47)$$

Once the membrane dimensions are limited of infinite, it may be observed how the group of equation shrinks on the HH equations. The parameters inside model just weren't appraised analytically. The values in the parameters were estimated by phenomenological methods through numerical experiments. It had been concluded that the dynamics forced with the equation is not reactive towards the constant parameter values.

The colored noise terms in equation (34) and equation (35) serve the purpose of capturing NCCP. The white terms in equation (40) - (42) match gate noise. The constant parameters of the model are:

$\gamma_k = 10$, $\omega_k^2 = 150$, T_k = 400, $\gamma_{Na} = 10$, ω_{Na}^2 = 200 and T_k = 800.

Chapter 6

RESULTS AND DISCUSSION

In this part, Güler model's (Güler, 2013) efficiency will be discussed through a series of tests, by monitoring the difference between Güler model, Fox and Lu equations and the microscopic simulations. The simple stochastic method was used as the microscopic simulations scheme (Zeng, 2004). This scheme applies Markovian process to simulate each gate individually, and continues for the rest of the gates. The input current in the simulations was a constant. The regular measure of spike train is called coefficient of variation (CV), this regularity measure is given by:

$$CV := \frac{\sqrt{\langle T^2\rangle - \langle T\rangle^2}}{\langle T\rangle} \tag{48}$$

$\langle T\rangle$: The mean interspike interval is given by equation:

$$\langle T\rangle = \lim_{N\to\infty} \frac{1}{N}\sum_i T_i \tag{49}$$

$\langle T^2\rangle$: The mean squared interval is given by equation:

$$\langle T^2\rangle := \lim_{N\to\infty} \sum (t_{i+1} - t_i)^2/N \tag{50}$$

The aim of this is to investigate the effect of the cross-correlation persistency placed in the trans-membrane voltage fluctuation by adding Güler model terms (Güler, 2013) into the conductance of the stochastic Hodgkin Huxley equations. A series of experiments are performed used to assess the Güler model effectiveness, in a comparative manner

with the Fox and Lu equations as well as with the microscopic simulations as mentioned before (Zeng, 2004); we can see through the results of the experiments that the spiking rate generated from the Güler model is very close to the one from the actual simulation, whatever the membrane size, was unlike the Fox and Lu equations which was far from the actual neuron spikes as shown in figure (6,8,10,12,14) with membrane size (402,801,1002,2700) potassium and (1340,2670,3340,9000) sodium. When we increase the input current with different membrane sizes, we can see in specific value of input current (8), with the membrane size exceeds (3500) potassium and (11670) sodium, the Fox and Lu curve becomes very closer to Güler model and microscopic simulations as shown in figure (16) .

Also we can see from the result of experiment are the coefficient of variation that generated from the Güler model has worked similarly to the microscopic simulations unlike Fox and Lu equations. Furthermore, when the membrane size is increased above 1002 potassium and 3340 sodium, it can be noticed that Fox and Lu equations reaches to the state of saturation. More like the saturation period is bounded with the value of input current between the value 0 and 4. In this area the coefficient of variation for Fox and Lu increase to the saturation state after that will return to the normal response as shown in figure (13, 15, 17, and 19).

Finally, we can notes from spike pattern figure (20) by comparing the voltage against the time variant for the three models, the Güler model is work with the microscopic simulation, dissimilar the Fox and Lu was work different from the microscopic simulation .

6.1 Technologies Used:

A computer program that solves the model eqns. (34, 35) numerically was developed by Güler. In the program, the input current was time independent which was modified so that the program could handle time dependent current .The model was developed by using C++ programming language and MATLAB was used for plotting the result.

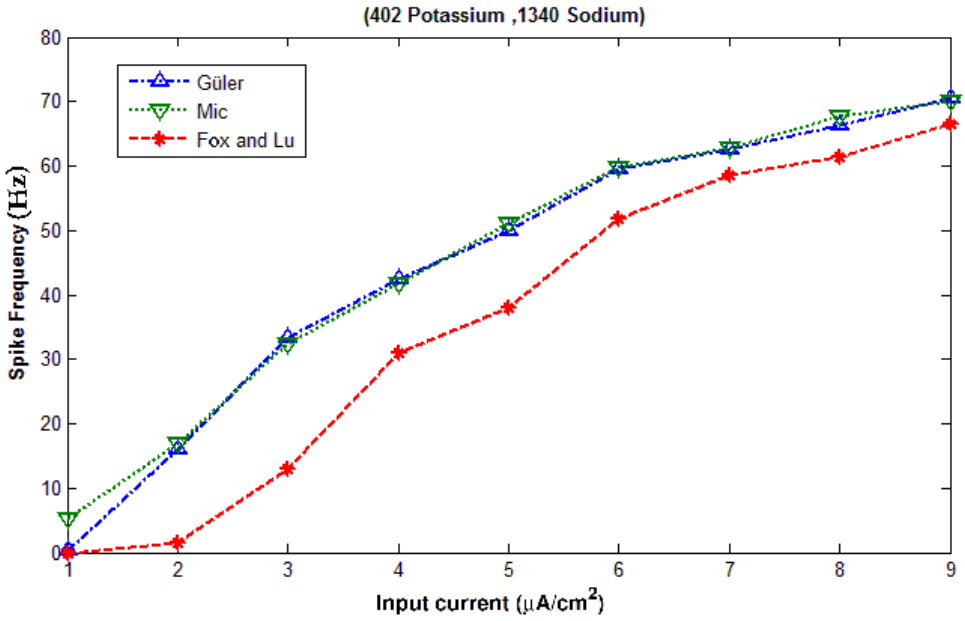

Figure 6: Mean spiking rates against the input current, displayed by a membrane patch of 402 potassium channels and 1340 sodium channels. The three plots shown correspond to Güler equations, the microscopic simulations, and the FL equations. The averages were computed over an 8 sec time window.

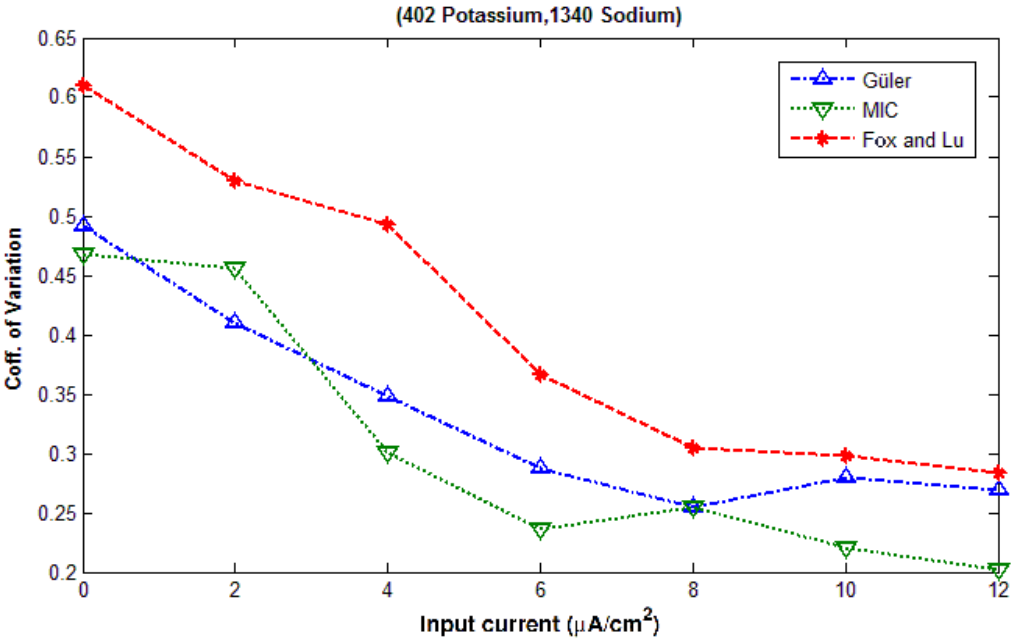

Figure 7: The coefficient of variation against the input current, displayed by a membrane patch of 402 potassium channels and 1340 sodium channels. The three plots shown correspond to Güler equations, the microscopic simulations, and the FL equations. The averages were computed over an 8 sec time window.

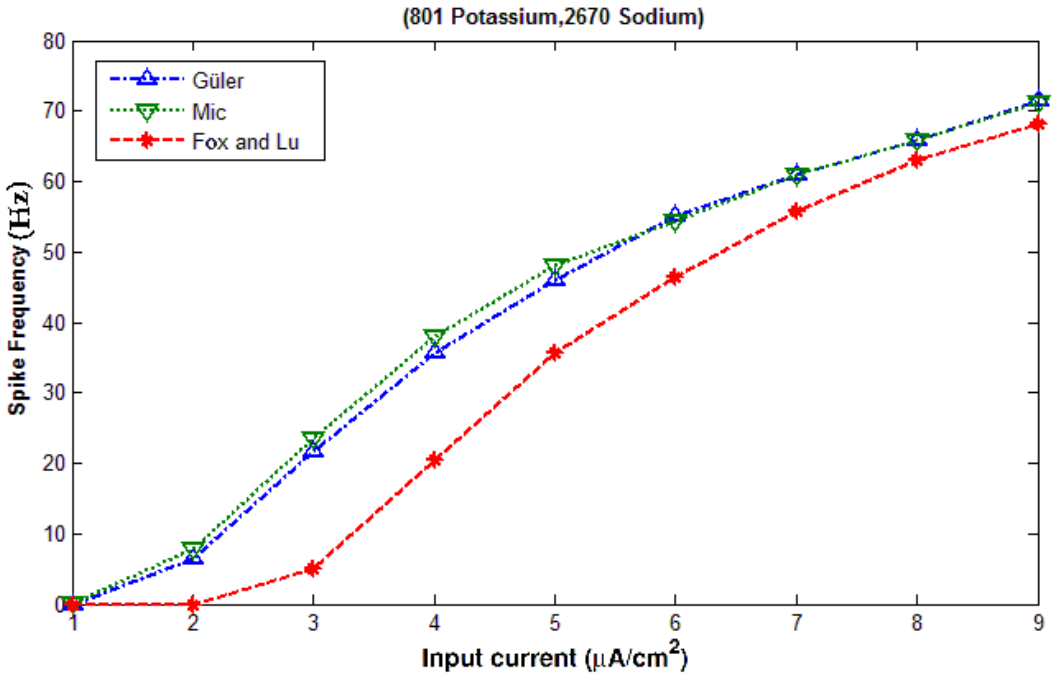

Figure 8: Same as Figure (6) but with the Membrane Patch 801 Potassium Channels and 2670 Sodium Channels.

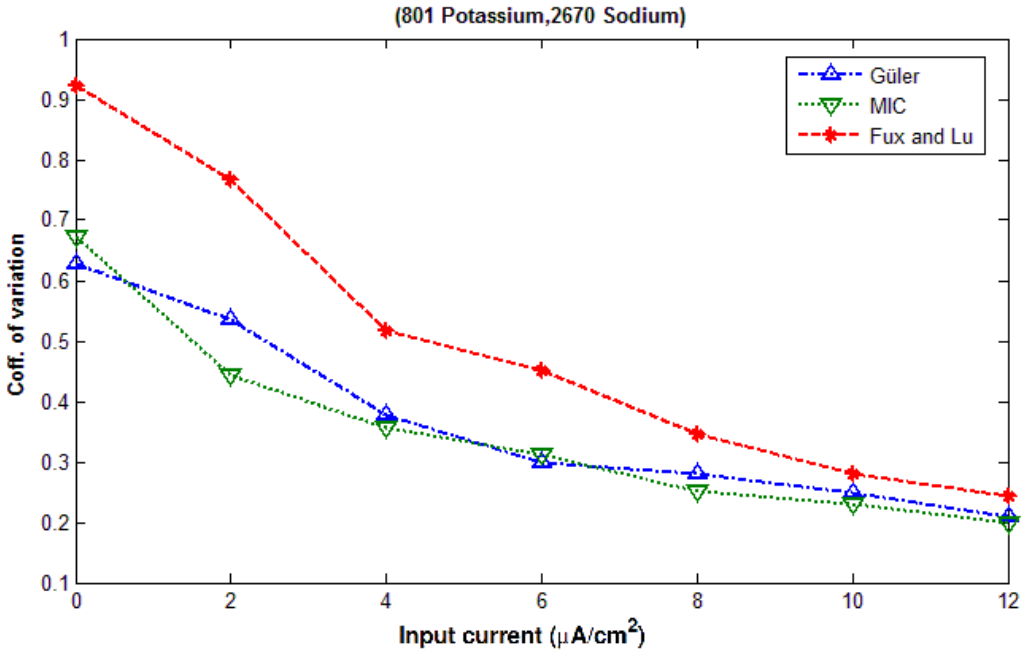

Figure 9: Same as Figure (7) but with the Membrane Patch 801 Potassium Channels and 2670 Sodium Channels.

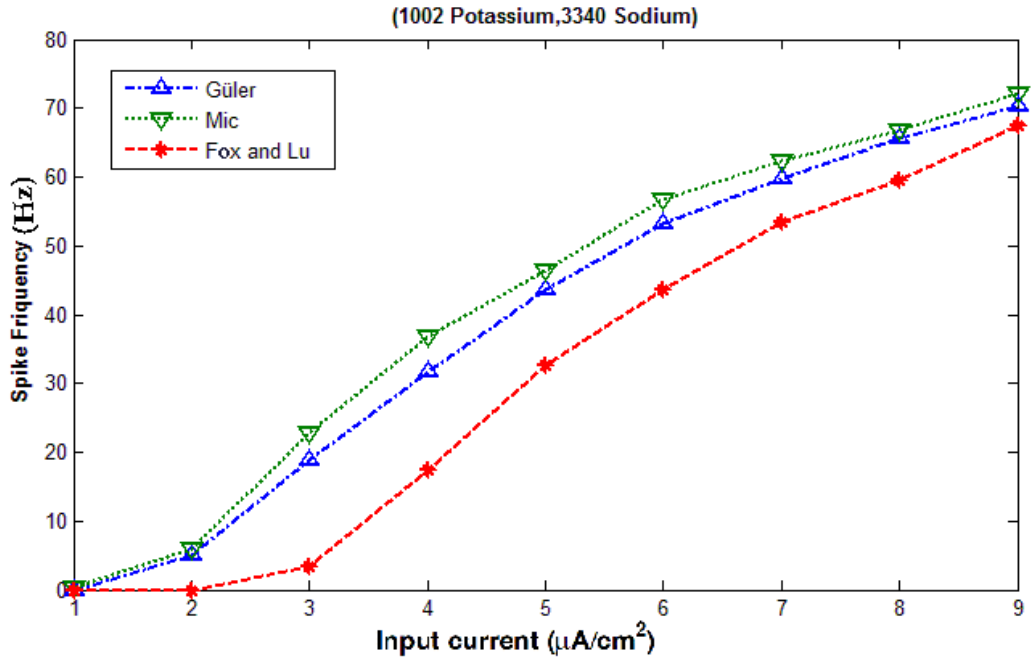

Figure 10: Same as Figure (6) but with the Membrane Patch 1002 Potassium Channels and 3340 Sodium Channels.

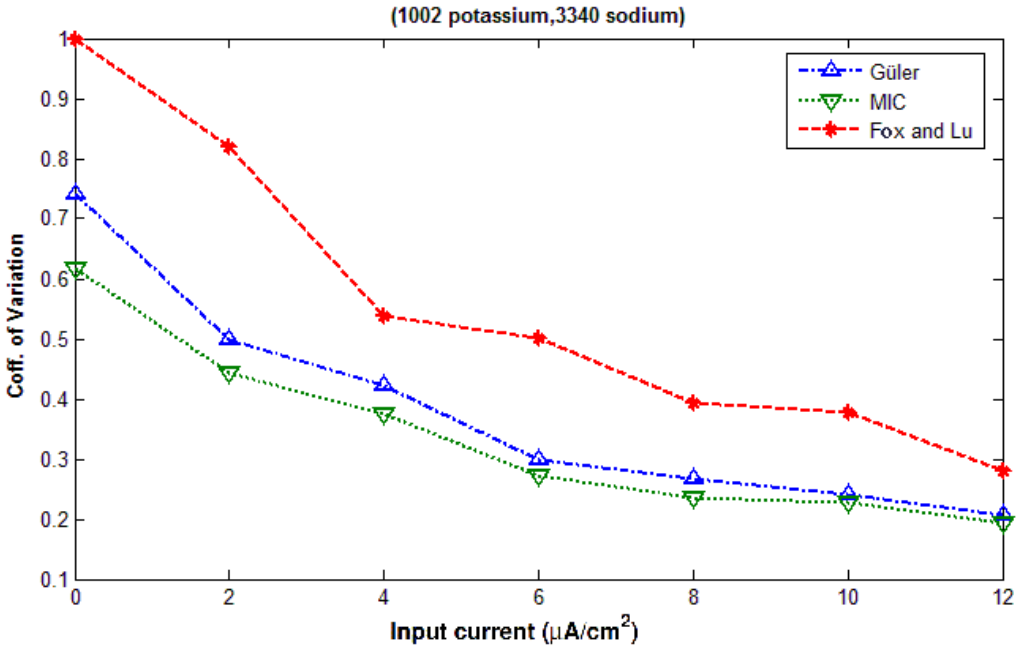

Figure 11: Same as Figure (7) but with the Membrane Patch 1002 Potassium Channels and 3340 Sodium Channels.

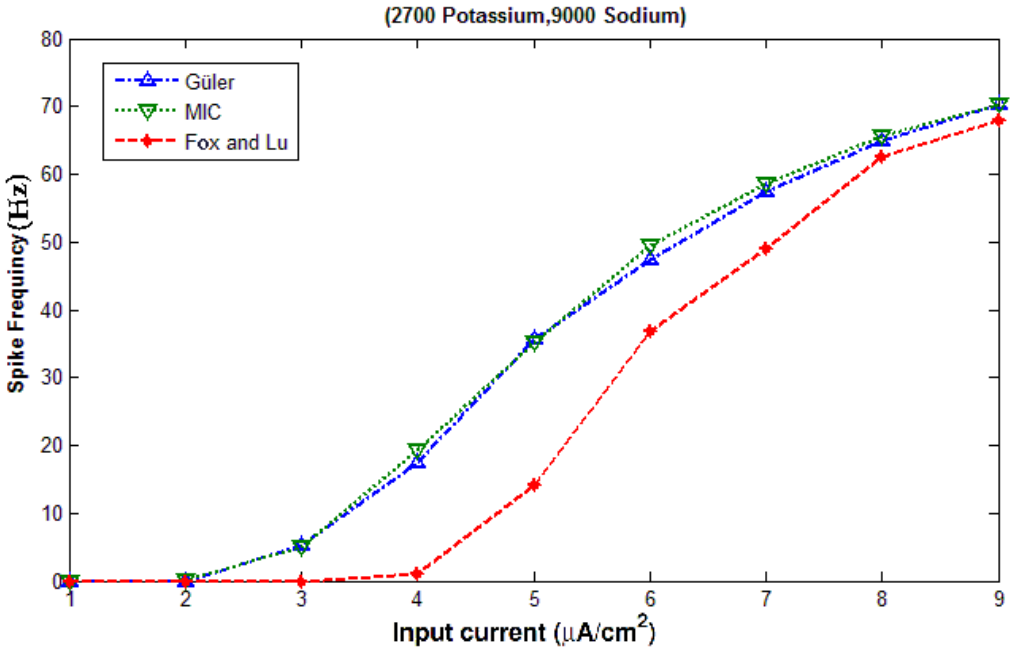

Figure 12: Same as Figure (6) but with the Membrane Patch 2700 Potassium Channels and 9000 Sodium Channels.

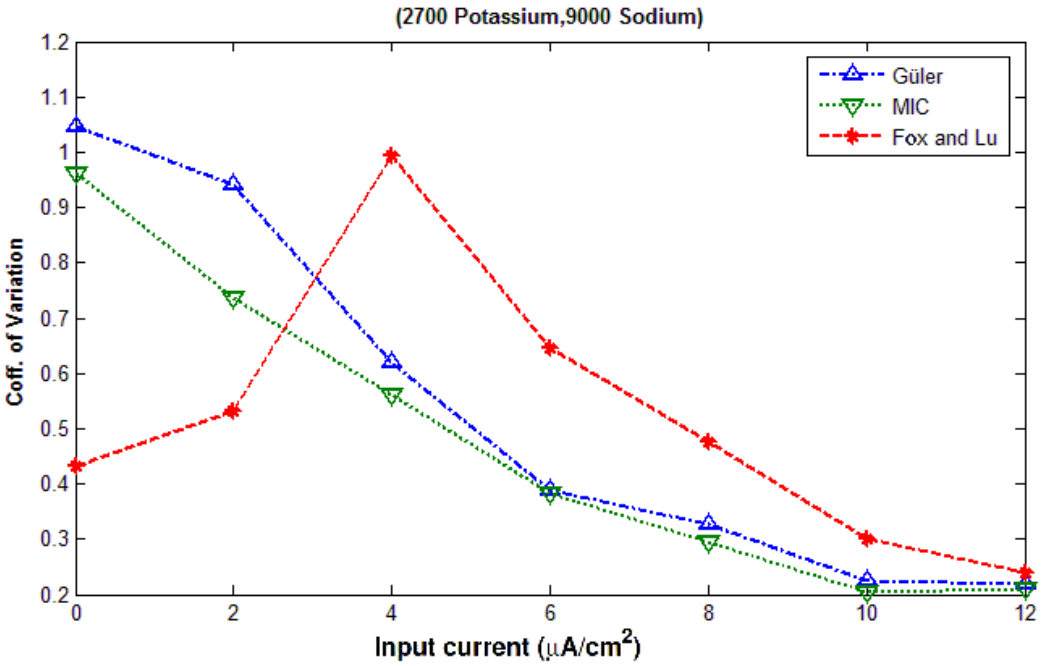

Figure 13: Same as Figure (7) but with the Membrane Patch 2700 Potassium Channels and 9000 Sodium Channels.

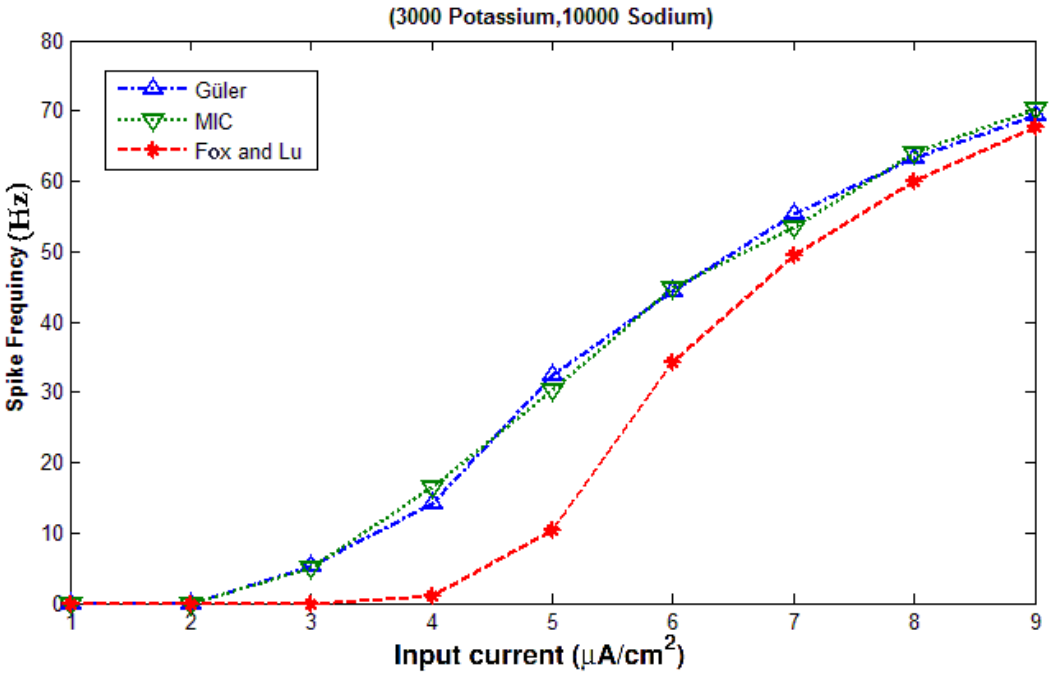

Figure 14: Same as Figure (6) but with the Membrane Patch 3000 Potassium Channels and 10000 Sodium Channels.

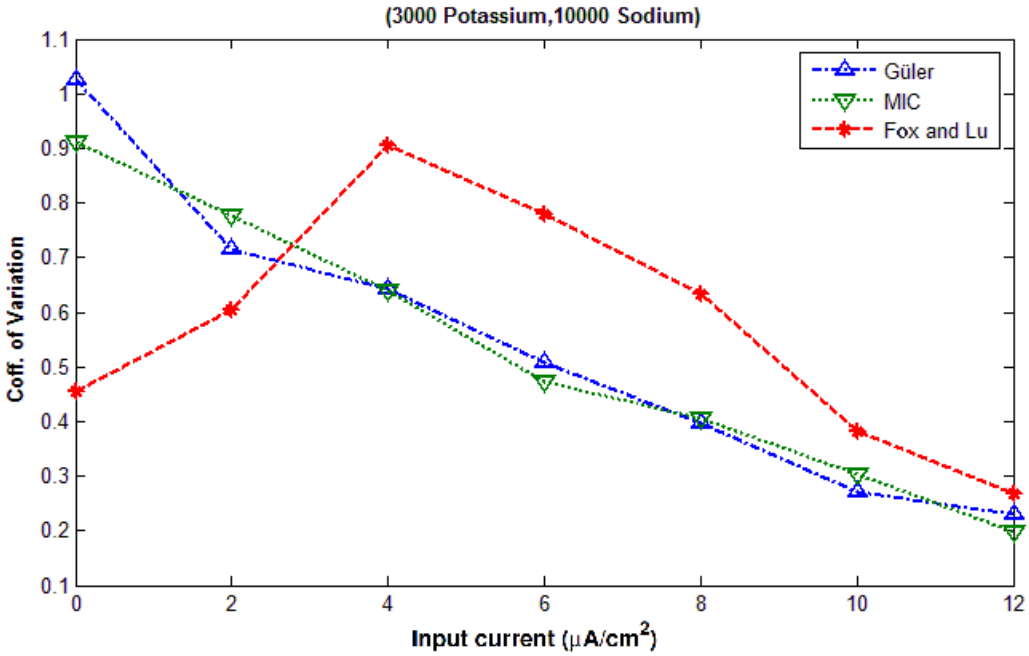

Figure 15: Same as Figure (7) but with the Membrane Patch 3000 Potassium Channels and 10000 Sodium Channels.

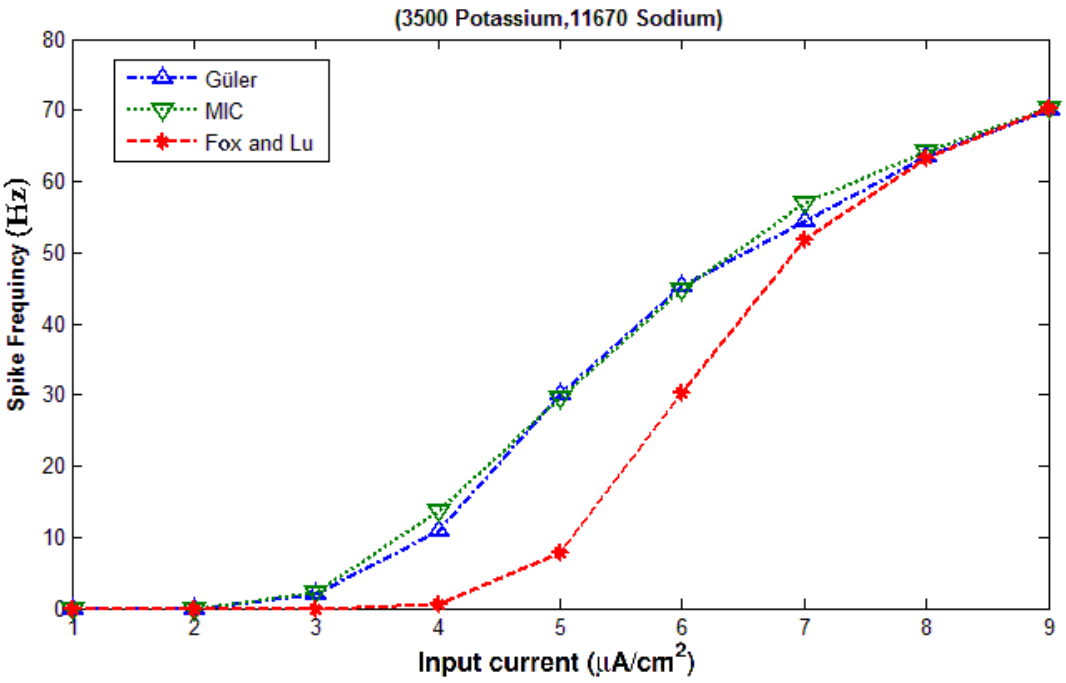

Figure 16: Same as Figure (6) but with the Membrane Patch 3500 Potassium Channels and 11670 Sodium Channels.

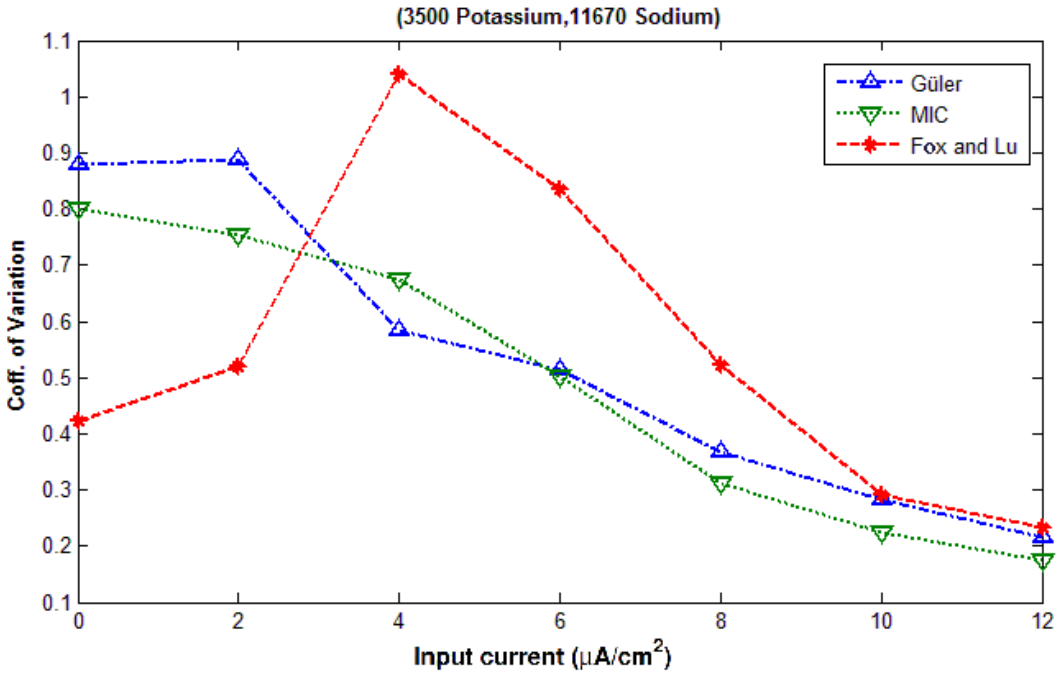

Figure 17: Same as Figure (7) but with the Membrane Patch 3500 Potassium Channels and 11670 Sodium Channels.

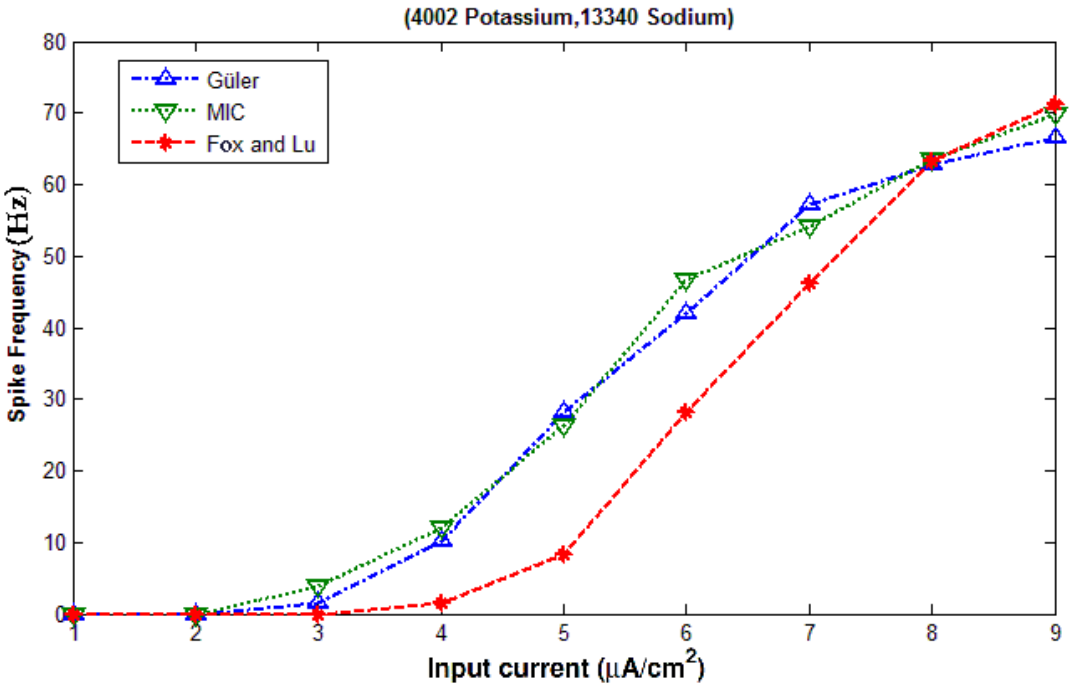

Figure 18: Same as Figure (6) but with the Membrane Patch 4002 Potassium Channels and 13340 Sodium Channels.

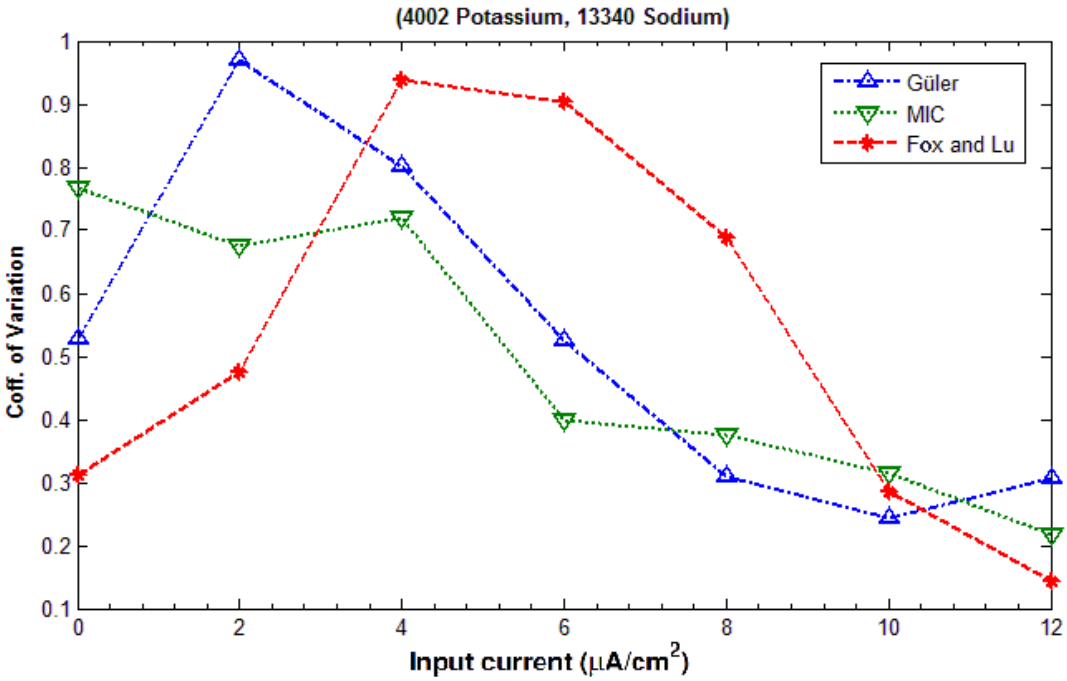

Figure 19: Same as Figure (7) but with the Membrane Patch 4002 Potassium Channels and 13340 Sodium Channels.

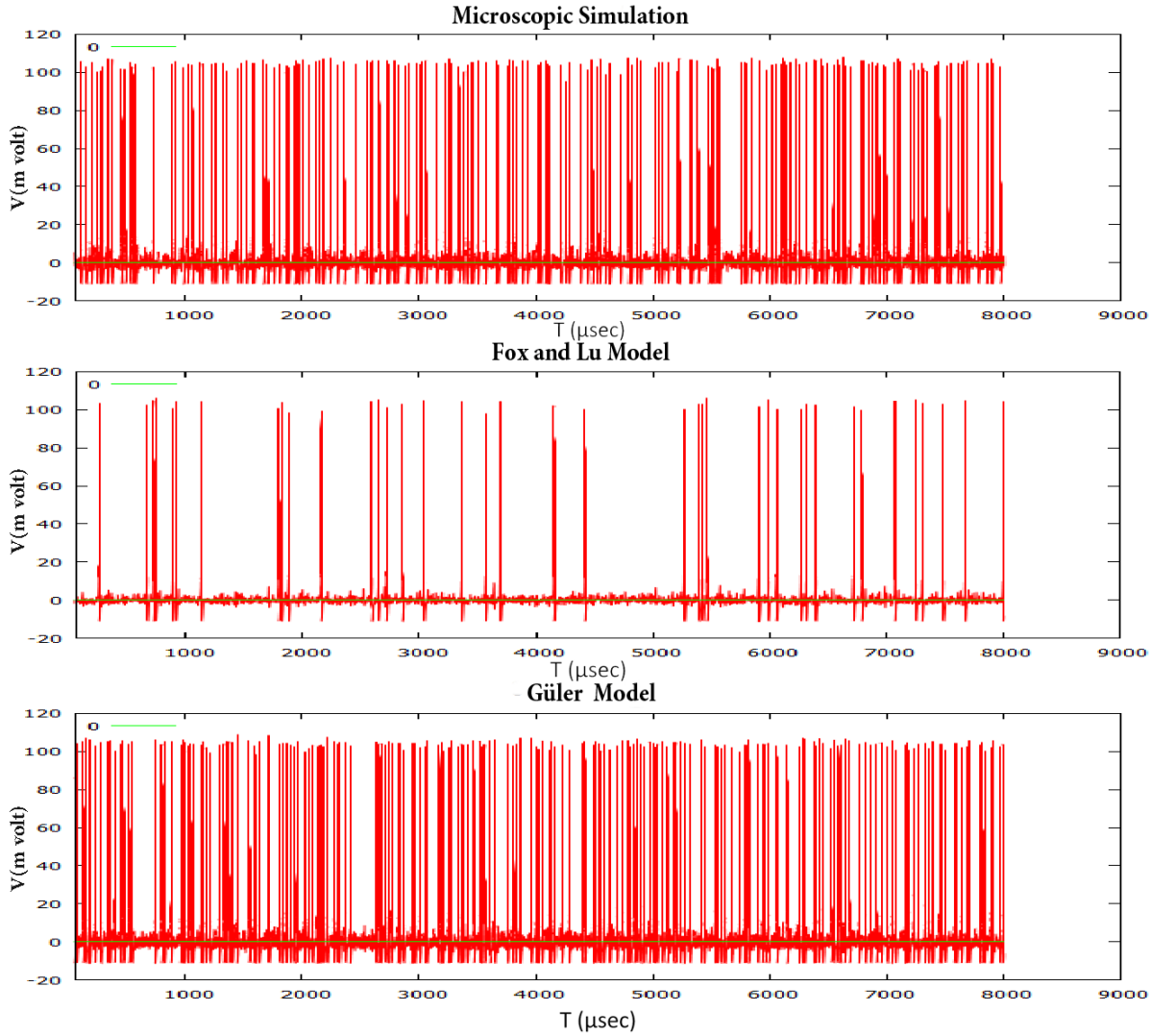

Figure 20: Spike pattern, the voltage against the time variant, displayed by a membrane patch of 801 potassium Channels and 2670 sodium channels with input current 6 $\mu A/cm^2$ .The three plots shown correspond to Güler equations, the microscopic simulations, and the FL equations.

Chapter 7

CONCLUSION

In this thesis, the colored noise neuron model was researched under the influence a set of input signals. In a recent study (Güler, 2011), it has been discovered that in the single ion channels, the multiplicity of the gates plays a crucial role which in turn motivates the NCCP (non-trivially cross correlation persistent) and also the last was found to be the key reason in the abnormal increases in the cell excitability as well as in the spontaneous firing in the small membrane size.

On top of that, it has been found that the NCCP keeps on promoting the spontaneous firing even if the membrane size is large anywhere the gate to noise which is definitely an inefficient for activating the cell. This study has also shown that the enhancement of the spike coherence has been brought on by the existence of the NCCP.

We investigated the effect of the cross-correlation persistency placed in the trans-membrane voltage fluctuation by adding Güler model terms (Güler, 2013) into the conductance of the stochastic Hodgkin Huxley equations. We performed a series of experiments to assess the Güler model's effectiveness, in a comparative manner with the Fox and Lu equations as well as with the Microscopic simulation as mentioned before (Zeng, 2004); We saw through the results of the experiments that the spiking rate generated from the Güler model is very close to the one from the actual simulations.

From the experiments standpoint, we conclude that Güler noise model handles the phenomenon in the NCCP properly and also we can easily see through the consequence of experiments that the spiking rate generated from the model is extremely near to the one from the actual simulation, regardless of a membrane size and input current , unlike the Fox and Lu equations which was away from the real neuron spikes specially when the input current is low. However, when we increase the input current with various membrane sizes we can begin to see that the Fox and Lu curve becomes closer to the Güler model and microscopic simulations.

REFERENCES

Abbot, D. P. (2002). theorretical Neuroscience Computation and mathematical modeling of neural system. MIT press.

Bezrukov, S. &. (1995). Noise-induced enhancement of signal transduction across voltage-dependent ion channels. Nature, 378, 362–364.

Chow, C. C. (1996). Spontaneous action potentials due to channel fluctuations. Biophysical Journal, 71,3013–3021.

DeFelice, L. J. (1992). Chaotic states in a random world: Relationship between the nonlinear differential equations of excitability and the stochastic properties of ion channels. Journal of Statistical Physics, 70, 339–354.

Dorval, A. D. (2005). Channel noise is essential for perithreshold oscillations in entorhinal stellate neurons. Journal of Neuroscience, 25, 10025–10028.

Faisal, A. A. (2007). Stochastic simulations on the reliability of action potential propagation in thin axons. PLoS Computational Biology, 3, e79.

Faisal, A. S. (2008). Noise in the nervous system. nervous system. Nature Reviews Neuroscience, 9, 292–303.

Fox R. F. and Y.N. Lu (1994). Emergent collective behavior in large numbers of globally coupled independently stochastic ion channels. Phys. Rev. E, 49: 3421-3431.

Güler, M. (2007). Dissipative stochastic mechanics for capturing neuronal dynamics under the influence of ion channel noise: Formalism using a special membrane. Physical Review E, 76,041918(17).

Güler, M. (2008). Detailed numerical investigation of the dissipative stochastic mechanics based neuron model. Journal of Computational Neuroscience, 25, 211–227.

Güler, M. (2011). Persistent membranous cross correlations due to the multiplicity of gates in ion channels. Journal of Computational Neuroscience ,31,713-724.

Güler, M. (2013). Stochastic Hodgkin-huxley equations with colored noise terms in the conductances. Neural Computation ,25,46-74.

Hille, B. (2001). Ionic channels of excitable membranes (3rd ed.). Massachusetts: Sinauer Associates.

Hodgkin, A. L. (1952). A quantitative description of membrane current and its application to conduction and excitationin in nerve. Journal of Physiology. (London.Print), 117, 500–544.

Izhikevich, E. M. (2007). Dynamical Systems in Neuroscience:The Geometry of Excitability and Bursting. San Diego, California.

Jacobson, G. A. (2005). Subthreshold voltage noise of rat neocortical pyramidal neurones. Journal of Physiology, 564,145–160.

Johansson, S. &. (1994). Single-channel currents trigger action potentials in small

cultured hippocampal neurons. Proceedings of National Academy of Sciences USA, 91, 1761–1765.

Jung, P. &. (2001). Optimal sizes of ion channel clusters. Europhysics Letters, 56, 29–35.

Koch, C. (1999). Biophysics of computation: Information processing in single neurons. Oxford: Oxford University Press.

Kole, M. H. (2006). Single Ih channels in pyramidal neuron dendrites: Properties, distribution, and impact on action potential output. Journal of Neuroscience, 26, 1677–1687.

Lynch, J. &. (1989). Action potentials initiated by single channels opening in a small neuron (rat olfactory receptor). Biophysical Journal, 55, 755–768.

N. A. Kako. (2013) An Investigation of the cofficient of variation using the colored stochastic Hodgkin-Hoxley equation .

Omer Hayman F. (2013) An investigation into the colored stochastic hodgkin-Huxley equation under time varying input currents.

Ochab-Marcinek, A. S. (2009). Noise-assisted spike propagation in myelinated neurons. Physical Review E, 79, 011904(7).

Özer, M. (2006). Frequency-dependent information coding in neurons with stochastic ion channels for subthreshold periodic forcing. Physics Letters A, 354, 258–263.

Rowat, P. F. (2004). State-dependent effects of Na channel noise on neuronal burst

generation. Journal of Computational Neuroscience, 16, 87–112.

Rubinstein, J. (1995). Threshold fluctuations in an N sodium channel model of the node of Ranvier. Biophysical Journal,68, 779–785.

Sakmann, B. &. (1995). Single-channel recording (2nded.). New York: Plenum.

Schmid, G. G. (2001). Stochastic resonance as a collective property of ion channel assemblies. Europhysics Letters, 56, 22–28.

Schneidman, E. F. (1998). Ion channel stochasticity may be critical in determining the reliability and precision of spike timing. Neural Computation, 10, 1679–1703.

Segev I., J. B. (2003). Cable and compartment models of dendritic trees in bower. the book of genesis 5:55.

Sigworth, F. J. (1980). The variance of sodium current fluctuations at the node of Ranvier. Journal of Physiology. (London Print), 307, 97–129.

Strassberg, A. F. (1993). Limitations of the Hodgkin–Huxley formalism: Effects of single channel kinetics on transmembrane voltage dynamics. Neural Computation 5, 843–855.

Whishaw, K. B. (2012). Fundamentals of Human Physiology FOURTH EDITION. Virginia United States.

White, J. A. (1998). Noise from voltage-gated ion channels may influence neuronal dynamics in the entorhinal cortex. Journal of Neurohysiology, 80, 262–269.

Zeng, S. &. (2004). Mechanism for neuronal spike generation by small and large ion channel clusters. Physical Review E, 70, 011903(8).